Primary-Dendrite Array: Observations from Ground-based and Space Station Processed Samples

Surendra N. Tewari – Cleveland State University
Ravi S. Rajamure – Cleveland State University*
Richard N. Grugel – Marshall Space Flight Center
Robert E. Erdman – The University of Arizona
David R. Poirier – The University of Arizona

Collaborative Effort between NASA and European Space Agency : Program MICAST

(Microstructure Formation in Castings of Technical Alloys under Diffusive and Magnetically Controlled Convective Conditions)

Introduction

- Why “low gravity” DS
- MICAST6 and MICAST 7 processing details
- Microstructure along DS length
- Primary dendrite spacing
- Primary dendrite trunk diameter
- Surprises

Dendritic array morphology depends upon DS processing parameters: G_l, R, C_o (convection?)

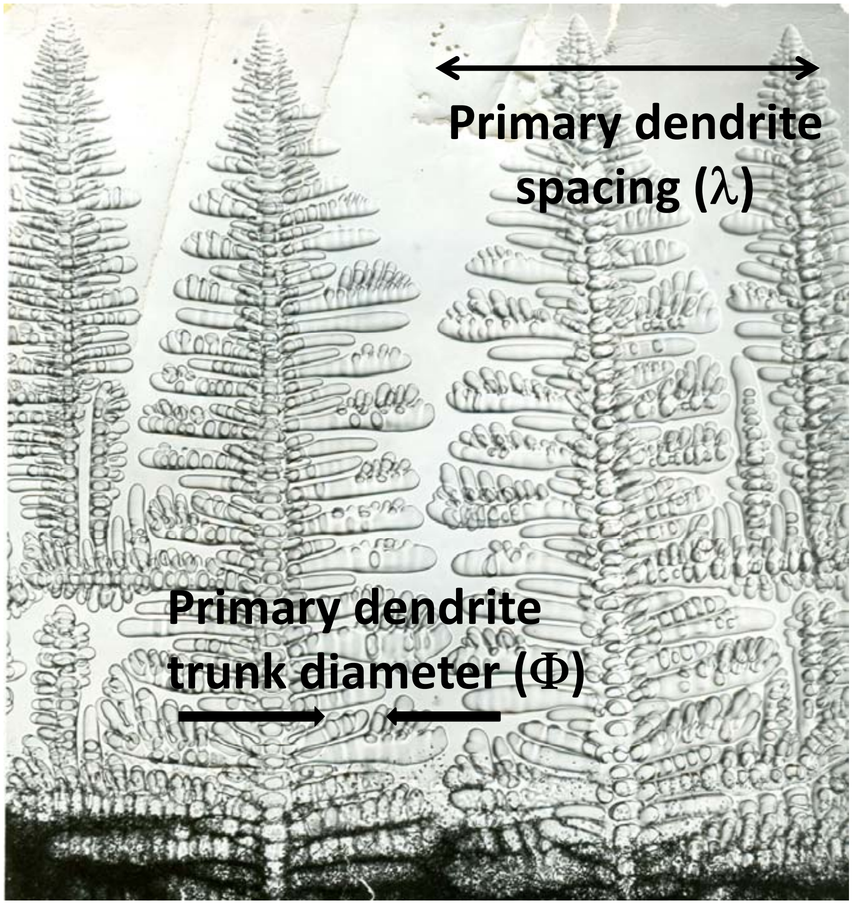

1. *Primary dendrite arm spacing (λ): Extensive literature (SCN/Metals)*
2. Secondary/tertiary arm spacing: Extensive-SCN/Metals
3. Dendrite tip radius: SCN/ limited (Al-Cu, Pb-Au, Pb-Pd)
4. Primary dendrite trunk diameter (Φ): Limited (Esaka:Thesis-86, Grugel: 92/95)

Natural convection Is inevitable during DS on earth

Thermally stable

- Solutally stable (Hypoeutectic Al-Cu)

"dendrite steepling" (radial macrosegregation)

- Solutally unstable (Hypoeutectic Pb-Sn)

"axial macrosegregation and freckle"

Dendritic array growth under diffusive solutal and thermal transport only possible in the absence of "g"

Purpose

MICAST: A systematic analysis of the effect of convection on the microstructural evolution in cast binary, ternary and commercial Al-Si based alloys.

MICAST6 ↓ MICAST 7

Re-melt and DS terrestrially grown dendritic mono-crystals of Al-7 wt% Si (9-mm dia, 25 cm long) in μg.

Advantages:	Minimize Thermo-Solutal Convection
Intent:	Produce Segregation Free Samples Grown Under Diffusion-Controlled Conditions
Purpose:	Better Understand the Relationship between Processing and Microstructure-Development

Microgravity Processing : Partially remelt and then DS from terrestrially grown dendritic mono-crystal in μg.

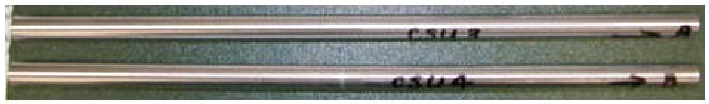

(Al-7%Si Single Crystal Dendritic)

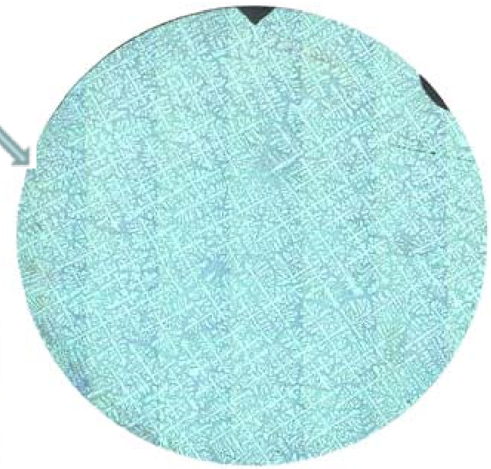

Transverse View

ESA- Sample Cartridge Assembly

ESA_MSL Low Gradient Furnace

ESA:
Material
Science
Laboratory

NASA_MSSR-1 Flight Rack

Microgravity Processed Sample MICAST 7

Eutectic Melt Back / Isotherm

X-ray radiograph of MICAST7

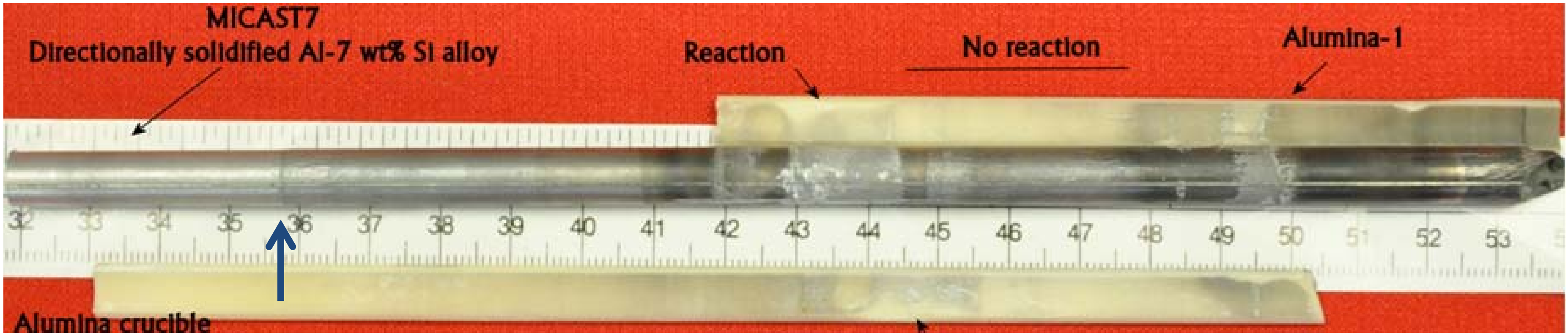

Eutectic Melt Back

MICAST6: ESA-Low Gradient Furnace (1-hr heat-up, 5-hr hold, G_l~ 20 K cm^{-1}): 3.8 cm at 5 $\mu m\ s^{-1}$, 11.3 cm at 50 $\mu m\ s^{-1}$

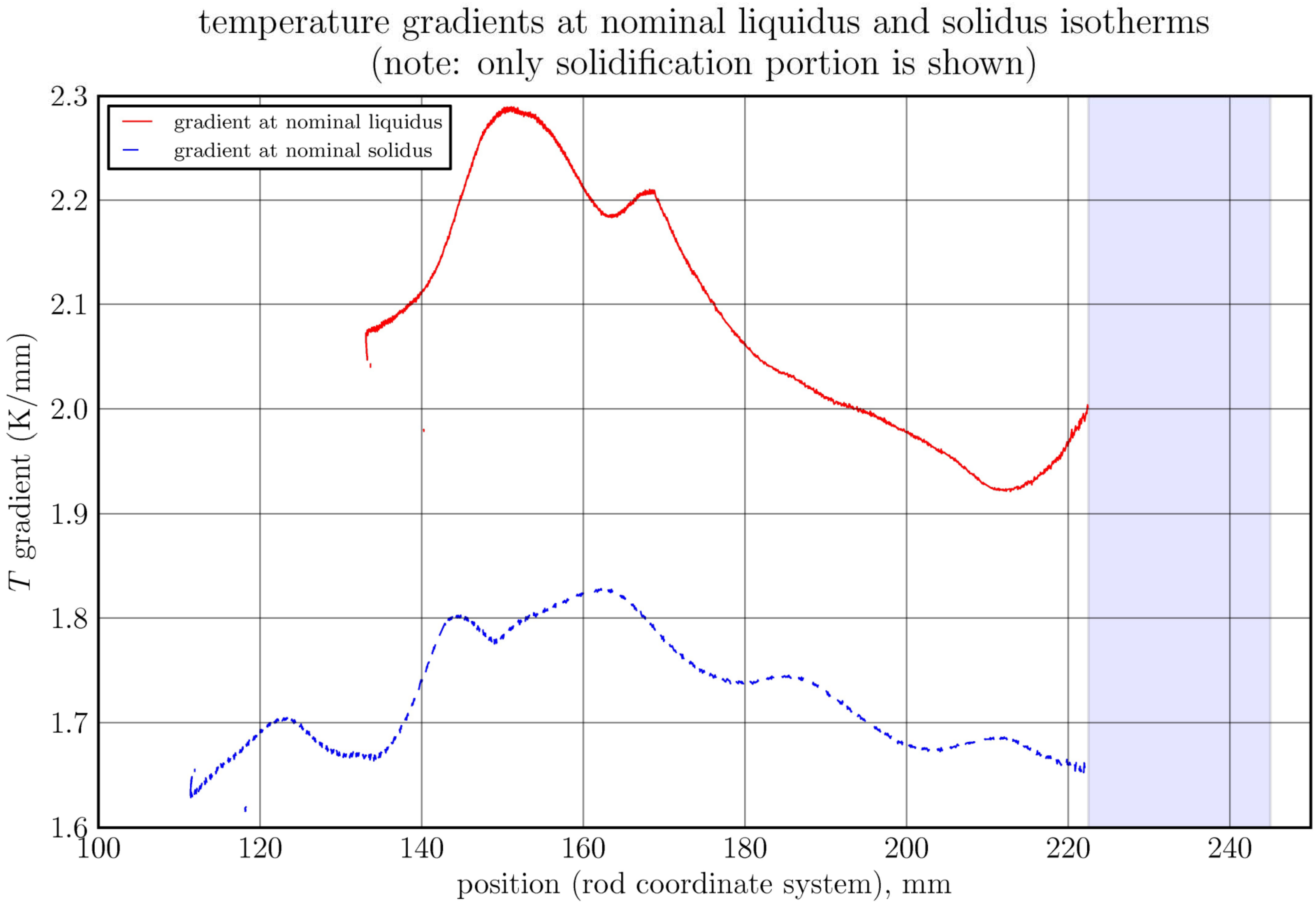

MICAST6: ESA-Low Gradient Furnace (1-hr heat-up, 5-hr hold, G_l~ 20 K cm^{-1}): 3.8 cm at 5 μm s^{-1}, 11.3 cm at 50 μm s^{-1}

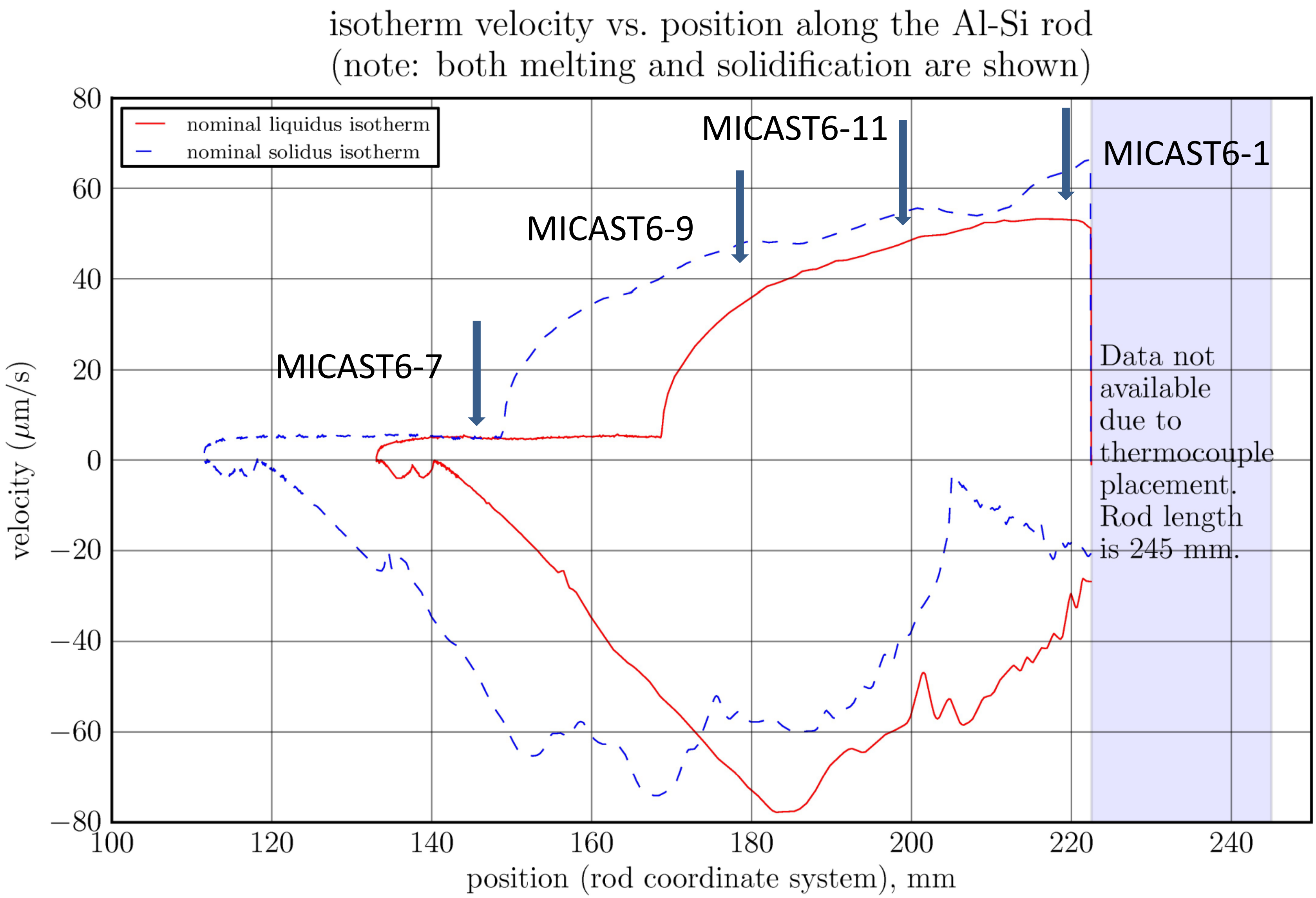

Comparison of microstructures: Al-7% Si directionally solidified on ground and on ISS (MICAST6)

MICAST6 SEED
41 K cm^{-1}, 22 μm s^{-1}

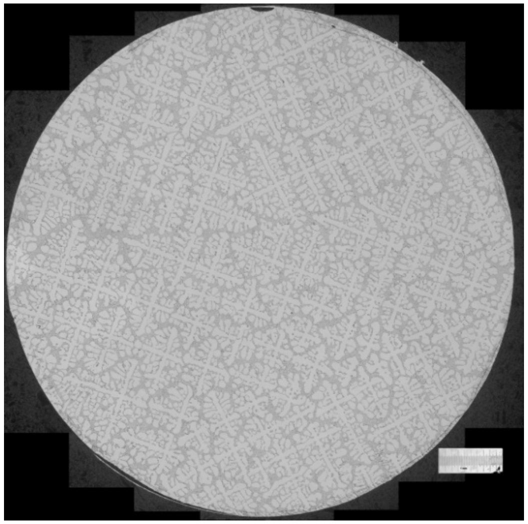

MICAST6: 20 K cm^{-1}

5 μm s^{-1}

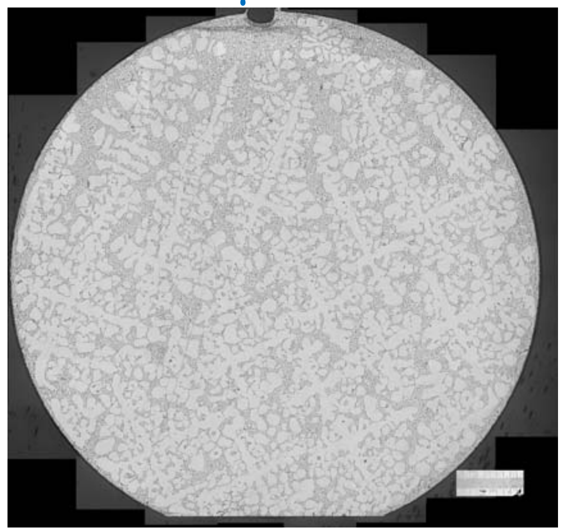

50 μm s^{-1}

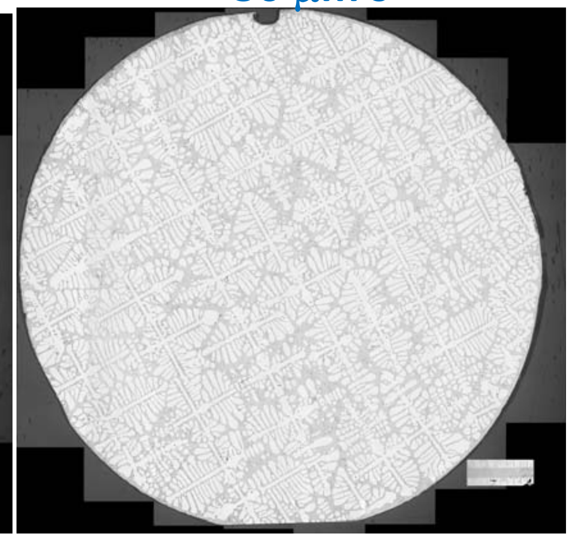

Terrestrial DS:
15 K cm^{-1} ➔

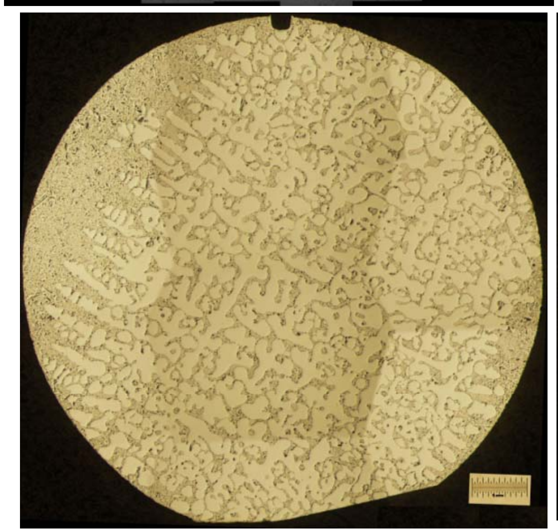

5 μm s^{-1}

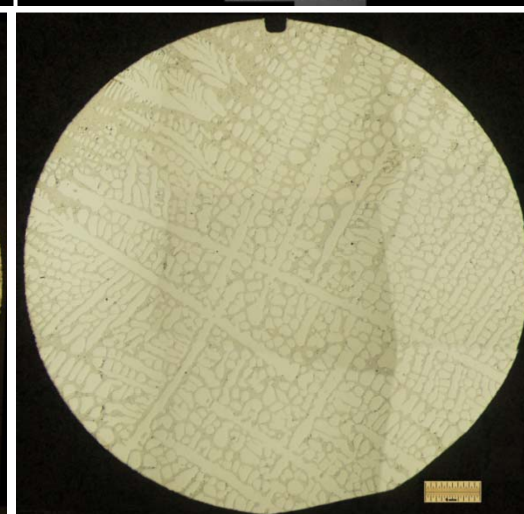

50 μm s^{-1}

Convection causes dendrite clustering (steepling) at low thermal gradient and growth speeds during terrestrial DS.

MICAST7: ESA-SQF (1-hr heat-up, 1-hr hold (G_l ~ 26 K cm^{-1}): 8.4 cm at 20 $\mu m\ s^{-1}$, 6.5 cm at 11 $\mu m\ s^{-1}$

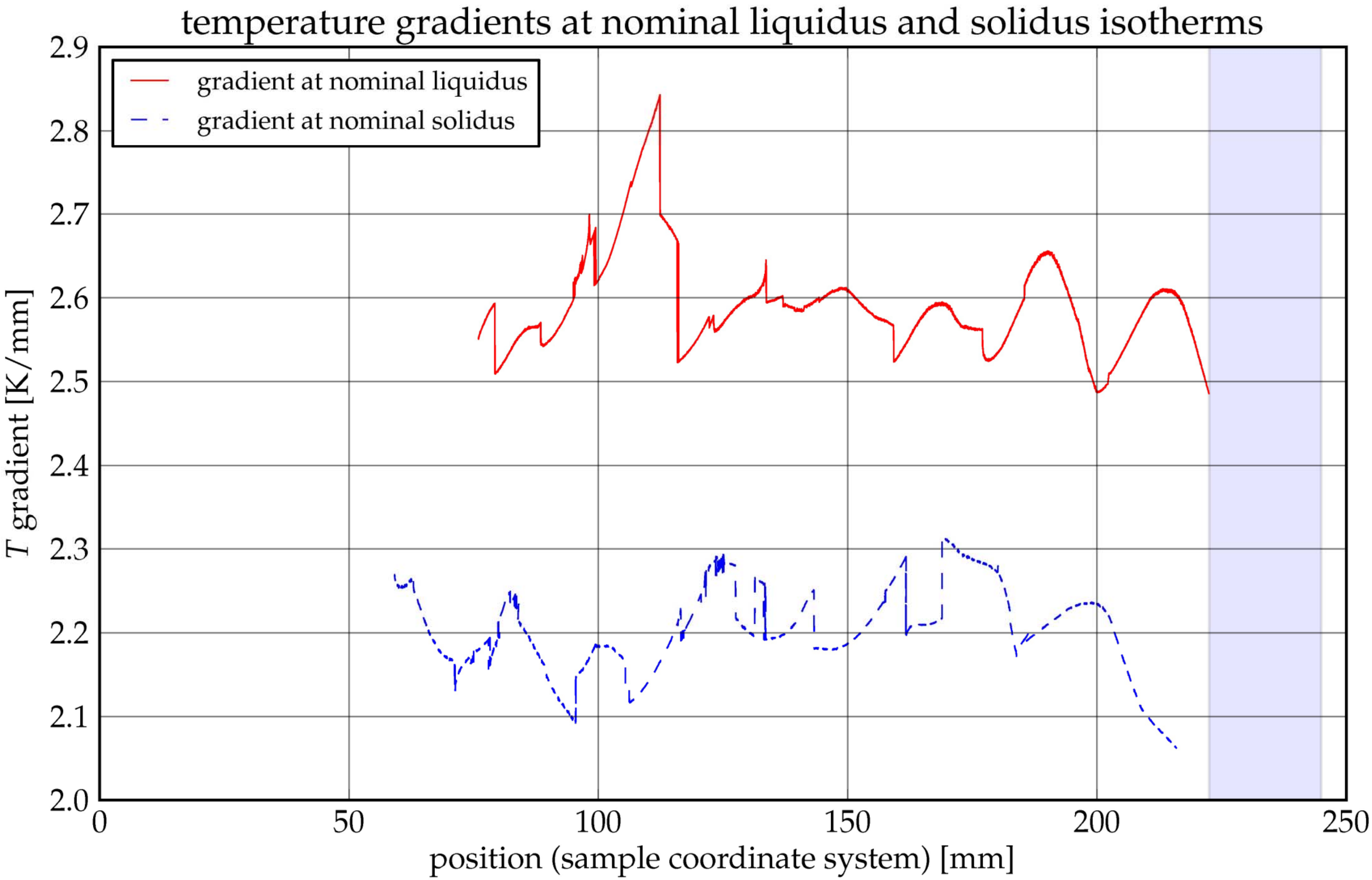

MICAST7: ESA-SQF (1-hr heat-up, 1-hr hold (G_l ~ 26 K cm^{-1}): 8.4 cm at 20 $\mu m\ s^{-1}$, 6.5 cm at 11 $\mu m\ s^{-1}$

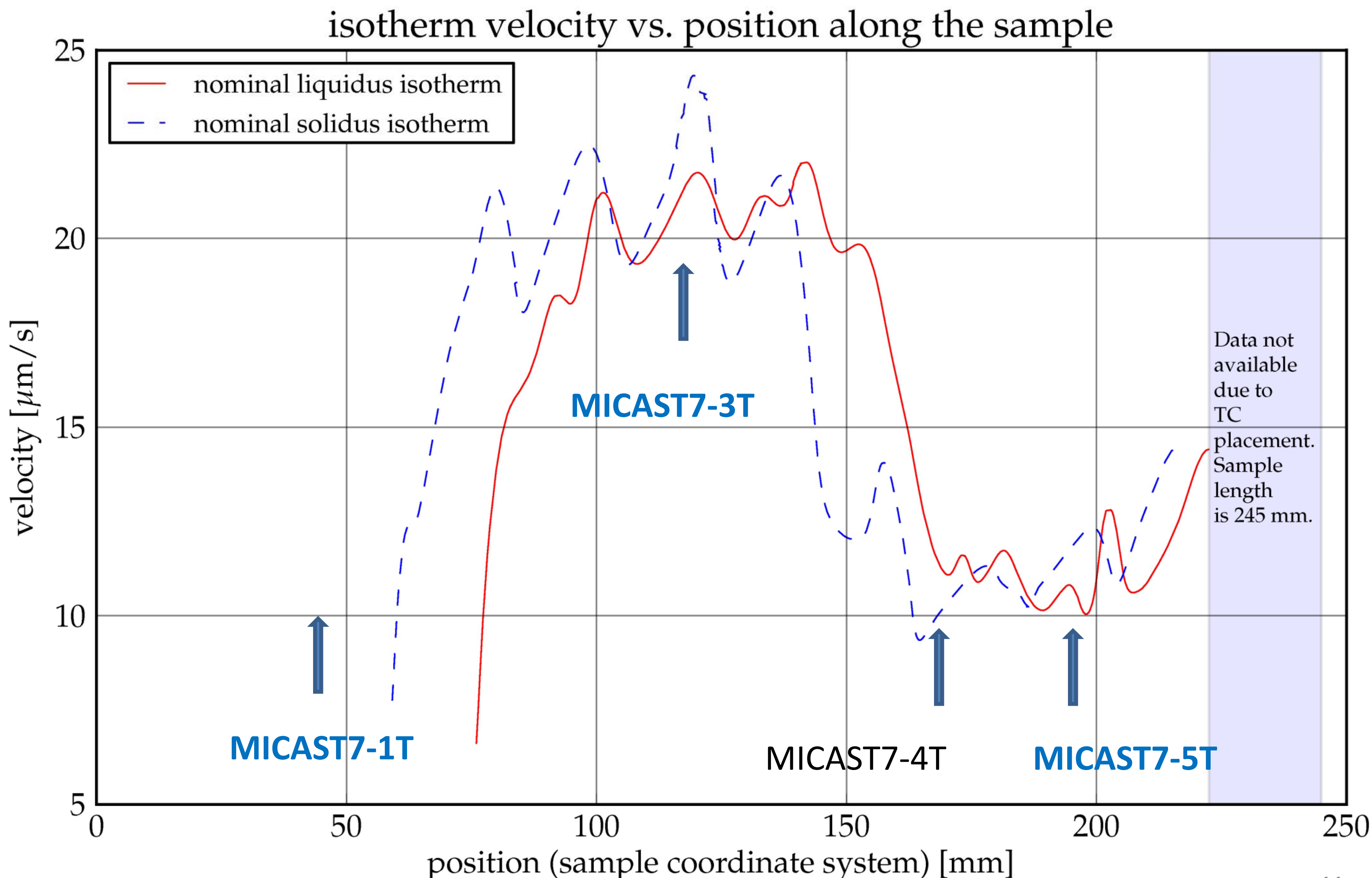

Comparison of microstructures: Al-7% Si directionally solidified on ground and on ISS (MICAST7)

MICAST7 SEED
41 K cm^{-1}, 22 μm s^{-1}

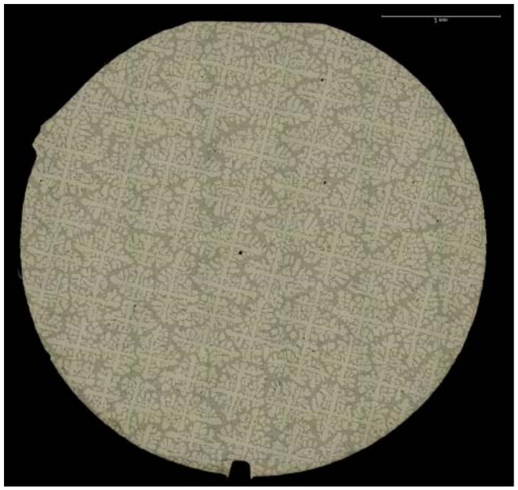

MICAST7: 26 K cm^{-1}

21 μm s^{-1}

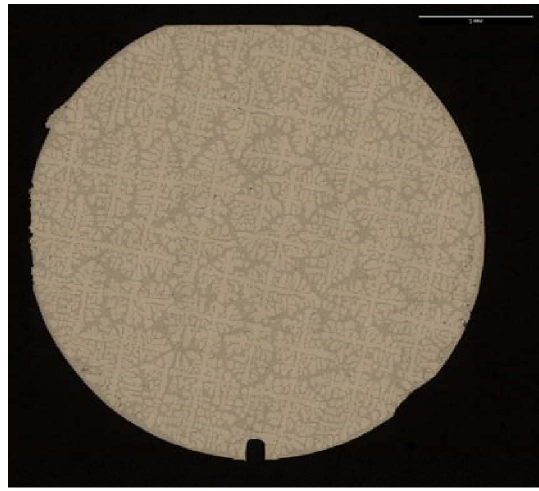

11 μm s^{-1}

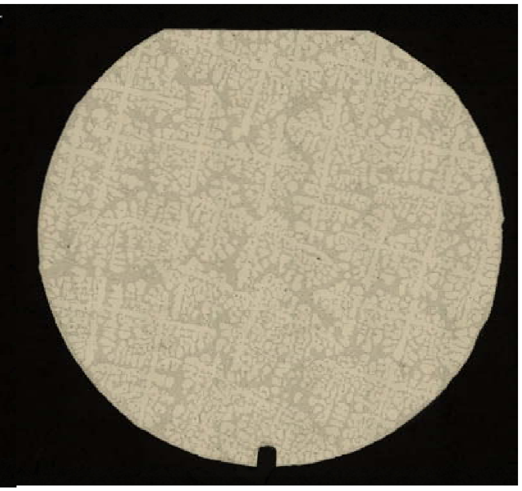

Terrestrial DS:
24 K cm^{-1} ➔

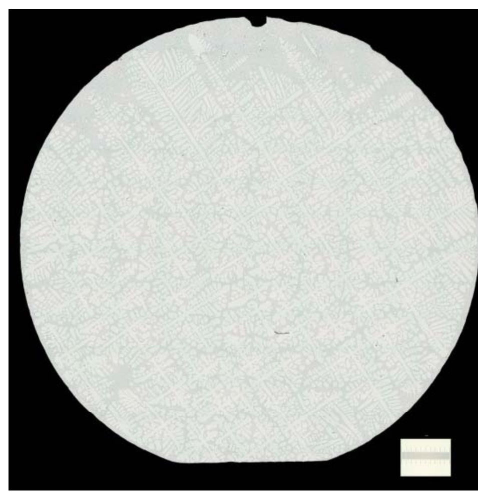

23 μm s^{-1}

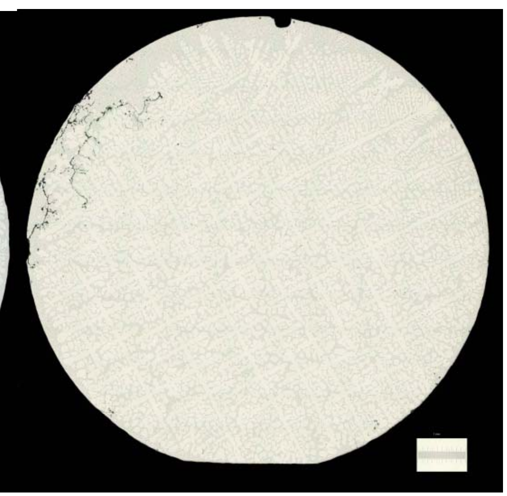

10 μm s^{-1}

Growth conditions for MICAST6 and MICAST 7 transverse microstructures examined

Sample ID	**G_l, K cm^{-1}**	**G_m, K cm^{-1}**	**R, μm s^{-1}**
MICAST6-1	19	18	52
MICAST6-11	20	18.5	47
MICAST6-9	21	19.3	34
MICAST6-7	22.8	20.4	5
MICAST7-3T	26	24	20
MICAST7-4T	26	24	11
MICAST7-5T	26	24	11

Theoretical models : Primary dendrite arm spacing (NEAREST NEIGHBOR SPACING)

$(m_l G_c^t - G_t)/(4\Pi^2 \Gamma T_m/r_t^2)=1$ for small $R r_t/2D_l$

$$r_t = -\frac{G_L \lambda_1^2}{4\sqrt{2}[m_L C_t (1-k) + \frac{D_L G_L}{R}]}$$

	Analytical	Numerical
Tip radius:	Trivedi (1980)	Hunt-Lu (1996)
Primary spacing:	Trivedi (1984)	Hunt- Lu (1996)

Physical Properties for Al- 7 wt% Si

Co	7 wt% Si	
m_l	-6.31 K/ wt% Si	Metals Handbook, vol 8(1973)
k	0.1	
Γ	0.196 μm K	Gunduz and Hunt (1985)
D_l	$4.3X10^{-9}$ m^2/s	(Poirier compilation)

Primary dendrite arm spacing compared with Trivedi calculations

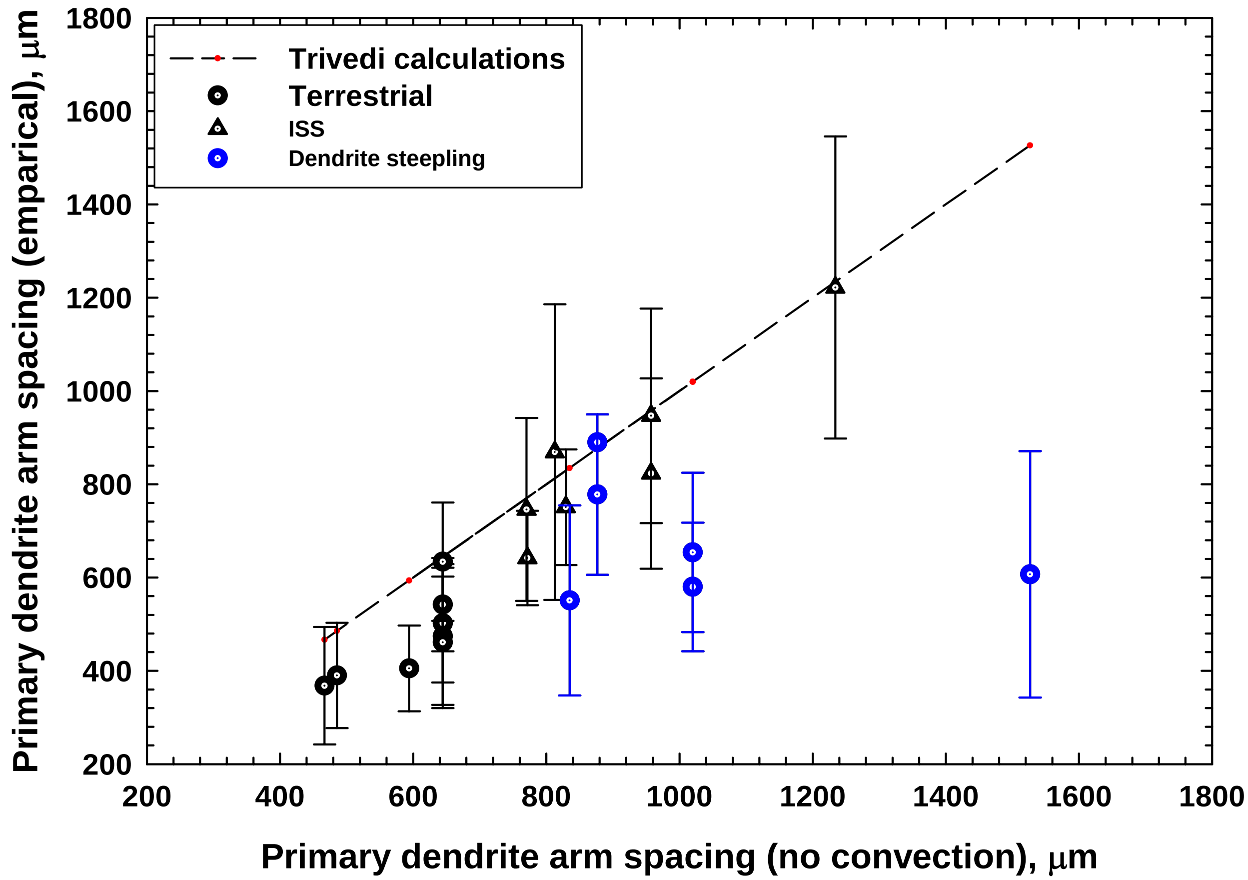

- ➢ISS-DS: Good agreement with predictions from Trivedi model .
- ➢Terrestrial DS ("Not steepled") : Good agreement with predictions from Trivedi model.
- ➢Terrestrial DS ("steepled"): Convection decreases primary dendrite arm spacing.

Primary dendrite arm spacing compared with Hunt-Lu calculations

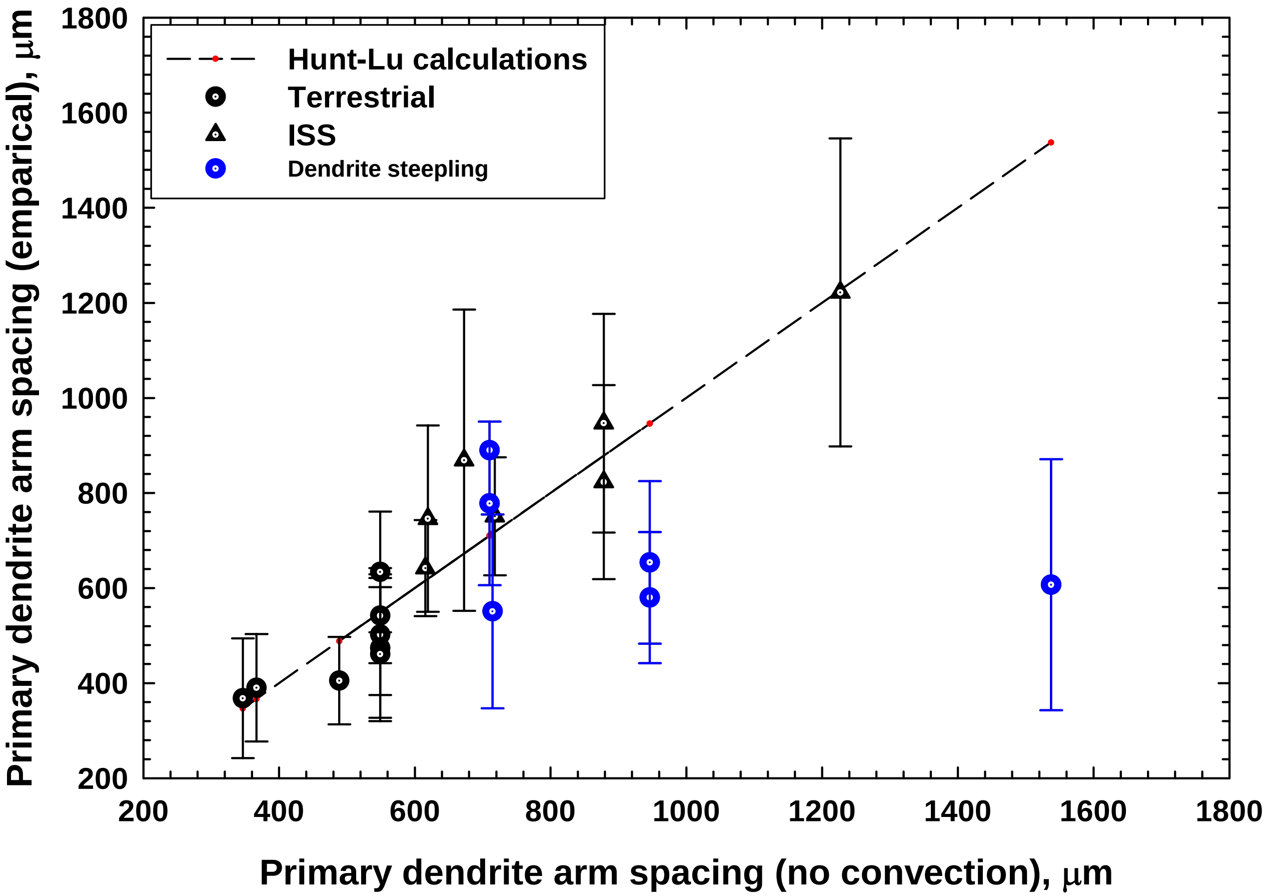

- ➢ **ISS-DS: Good agreement with predictions from Hunt-Lu model.**
- ➢ **Terrestrial DS ("Not steepled") : Good agreement with predictions from Hunt-Lu model.**
- ➢ **Terrestrial DS ("steepled"): Convection <u>decreases</u> primary dendrite arm spacing.**

No theoretical model for Primary dendrite trunk diameter (ϕ)

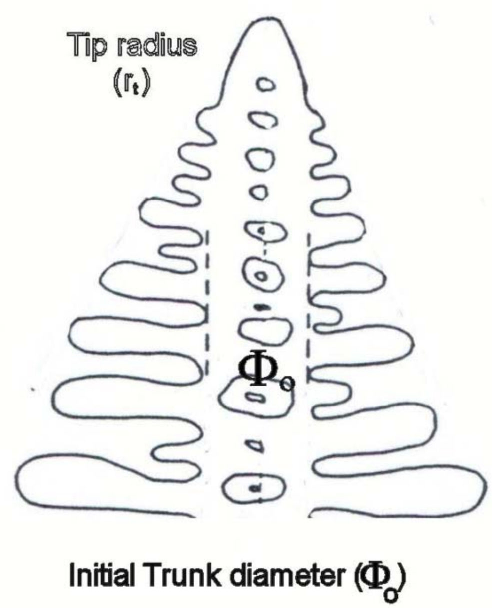

Esaka Thesis (1986): Trunk diameter increases rapidly near the tip till ~ 10 side-branch formations. He measured this initial trunk diameter (ϕ_o). Eighty DS experiments (four SCN-Acetone alloys grown with various R and G_l)

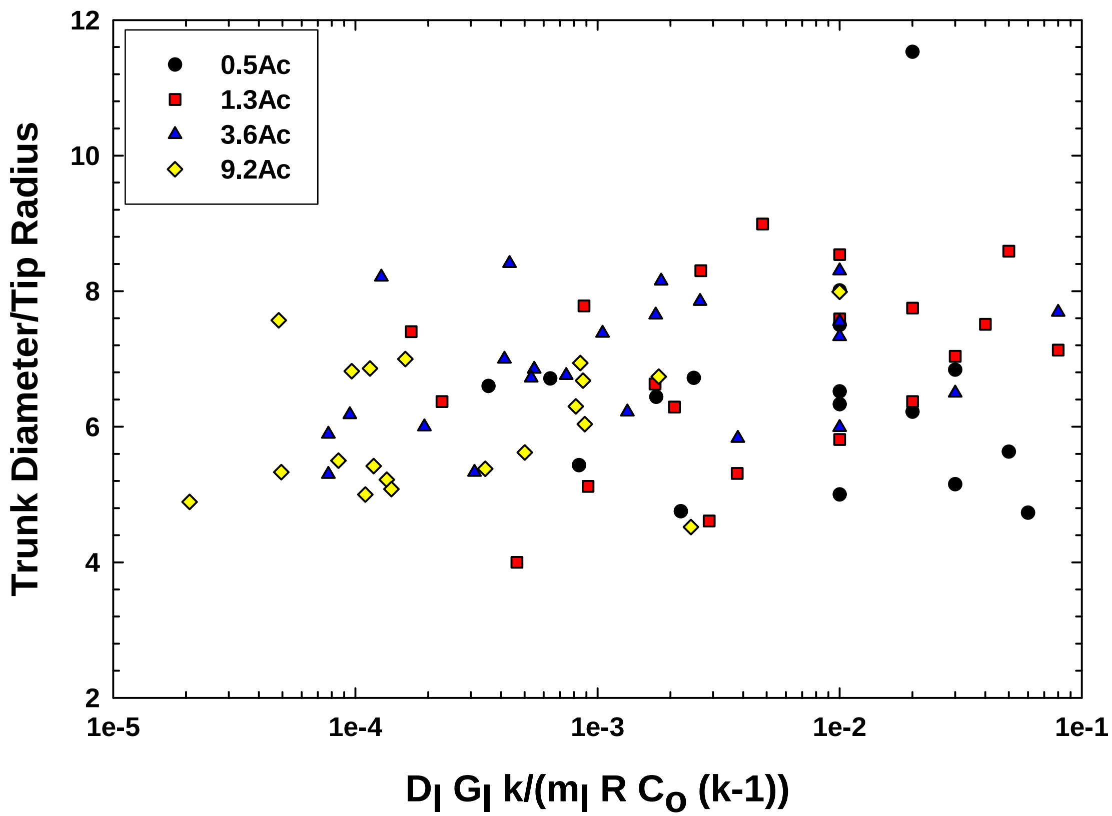

$D_l G_l k/(m_l R C_o (k-1))$]: More branched dendritic morphologies will be located towards the left, and less-branched/cellular towards the right side of the X-axis.

(Initial trunk diameter (ϕ_o)/tip radius) = 6.59±1.3

Primary dendrite trunk diameter (ϕ) model

1. The trunk diameter (ϕ) increases rapidly near the tip till time, **t_o= 22*r_t/R**), when $\phi = \phi_o$ = **6.59 r_t** (paraboloidal envelope near tip).

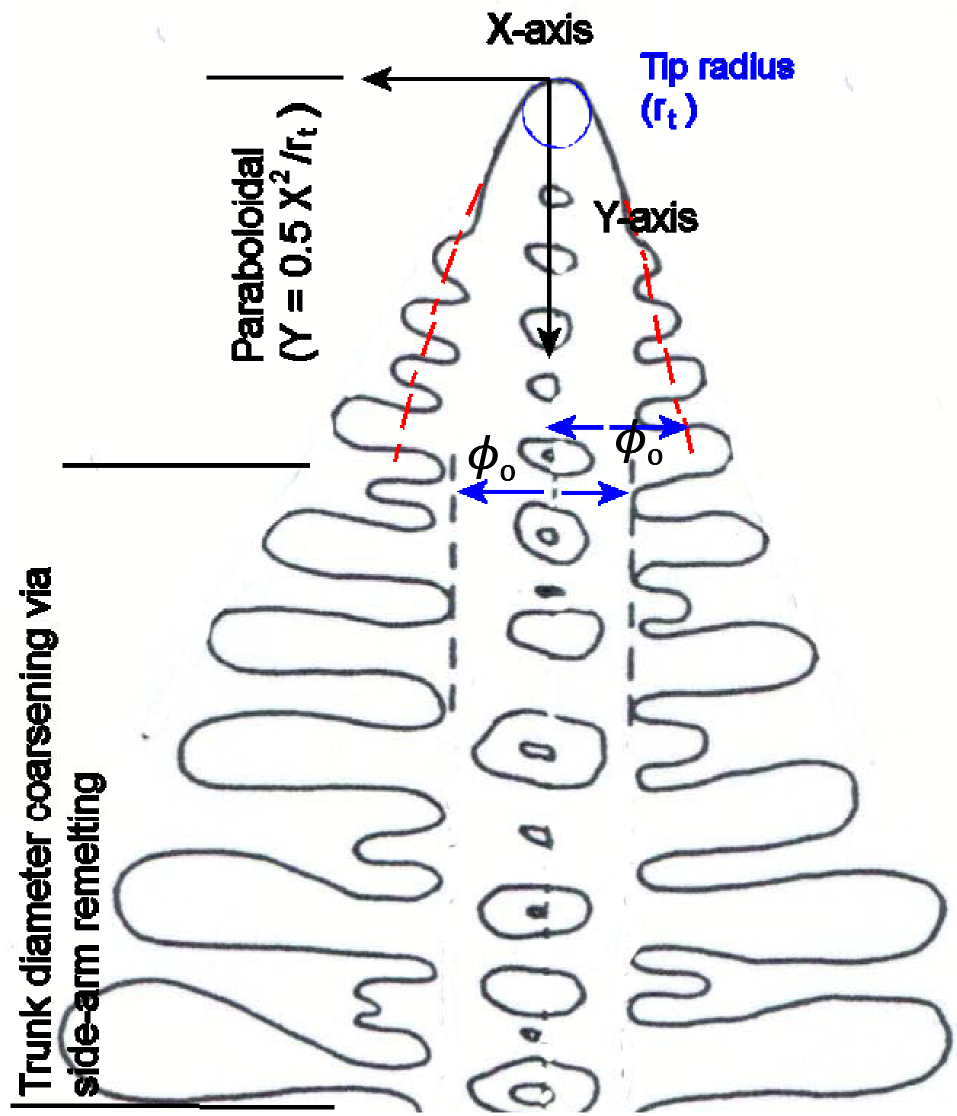

Primary dendrite trunk diameter (ϕ) model

2. After t_o the trunk diameter increases via remelting of 4-side arms (r) and deposition of melted arm material on "trunk surface "over length h" = ϕ.

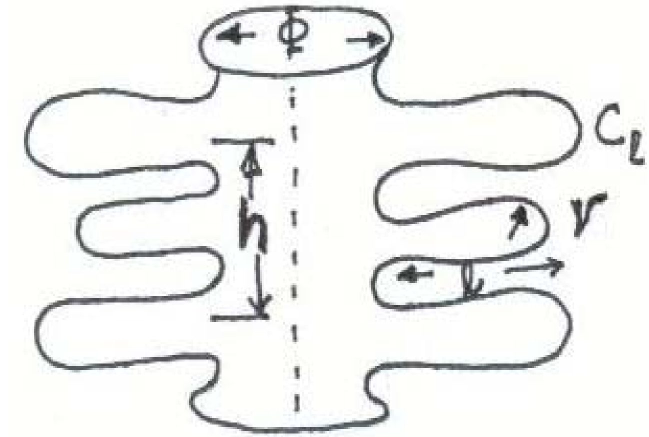

Assumptions:

1. Kirkwood model (1985) of ripening applies.
2. Secondary arm melts back because of its curvature.
3. Mass of the melted arm deposits on trunk surface where there is negative curvature.

$$\frac{dl}{dt} = \frac{4\, D_l\, \Gamma}{m_l\, C_l\, (1-k)\, r^2} \quad (1)$$

$$\pi \phi h \frac{d\phi}{2\, dt} = 4 * \pi r^2 \frac{dl}{dt} \quad (2)$$

$$C_l = C_o + R\, G_m\, t/m_l \quad (3)$$

$$\phi^2 \frac{d\phi}{dt} = 32 \frac{D_l\, \Gamma}{m_l\ (1-k)(\, C_o + \frac{R\, Gm\, t}{m_l})} \quad (4)$$

Primary dendrite trunk diameter (ϕ) model

$$\phi^3 = 96\,\frac{D_l\,\Gamma}{RGm\ (1-k)}\ln\left\{\frac{\left(1+\dfrac{R\,Gm\ t}{m_l C_o}\right)}{\left(1+\dfrac{R\,Gm\ t_o}{m_l C_o}\right)}\right\} + \Phi_o^3$$

Mushy zone freezing time $\sim$ $m_l(C_E\text{-}C_o)/RG_m$

Use tip radius (r_t) predicted from Trivedi (1980) or Hunt-Lu (1996) models to get the initial trunk diameter ϕ_o = 6.59 r_t in order to predict the processing parameter dependence of "Primary dendrite trunk diameter" from above relationship.

Primary dendrite trunk diameter as compared to trunk diameter model calculations, using r_t (Trivedi)

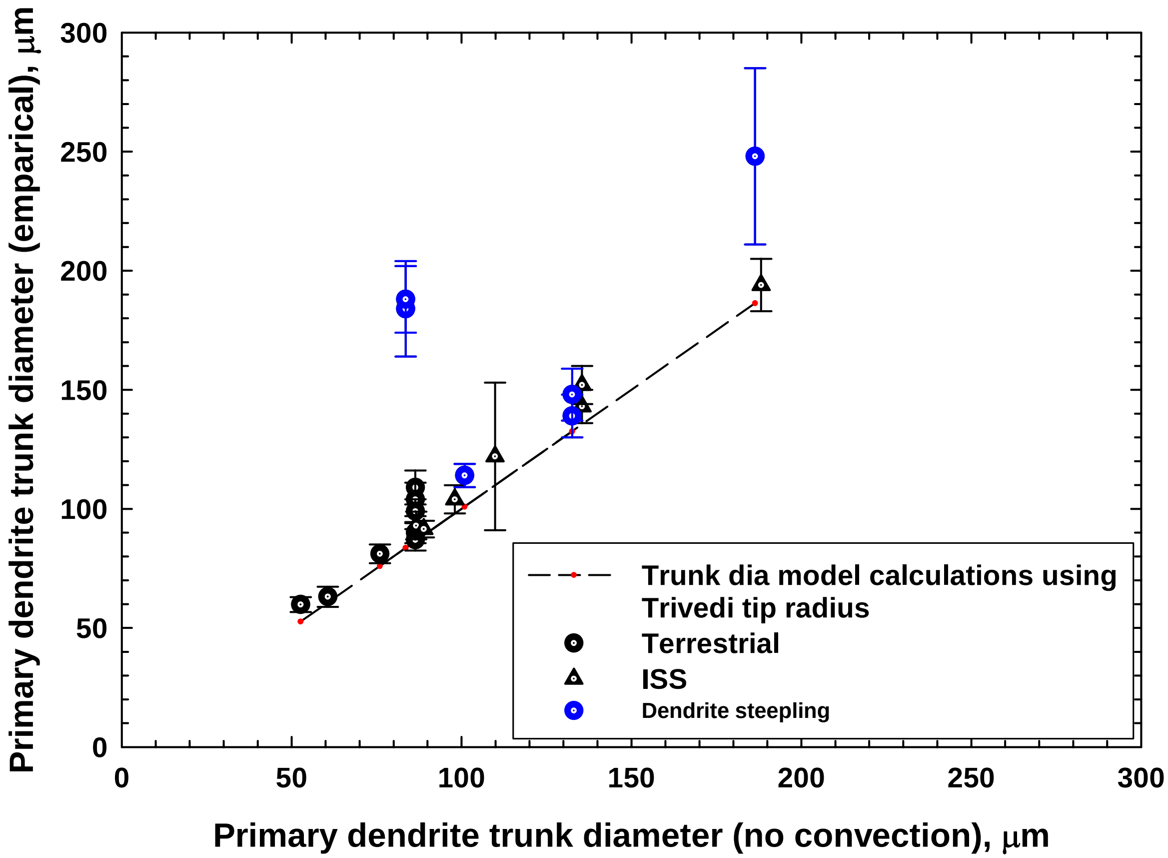

- ➢ISS-DS: Good agreement with predictions from the trunk-diameter model.
- ➢Terrestrial DS (“Not steepled”) : Good agreement with predictions from model.
- ➢Terrestrial DS (“steepled”): Convection <u>increases</u> trunk diameter.

Primary dendrite trunk diameter as compared to trunk diameter model calculations, using r_t (Hunt-Lu)

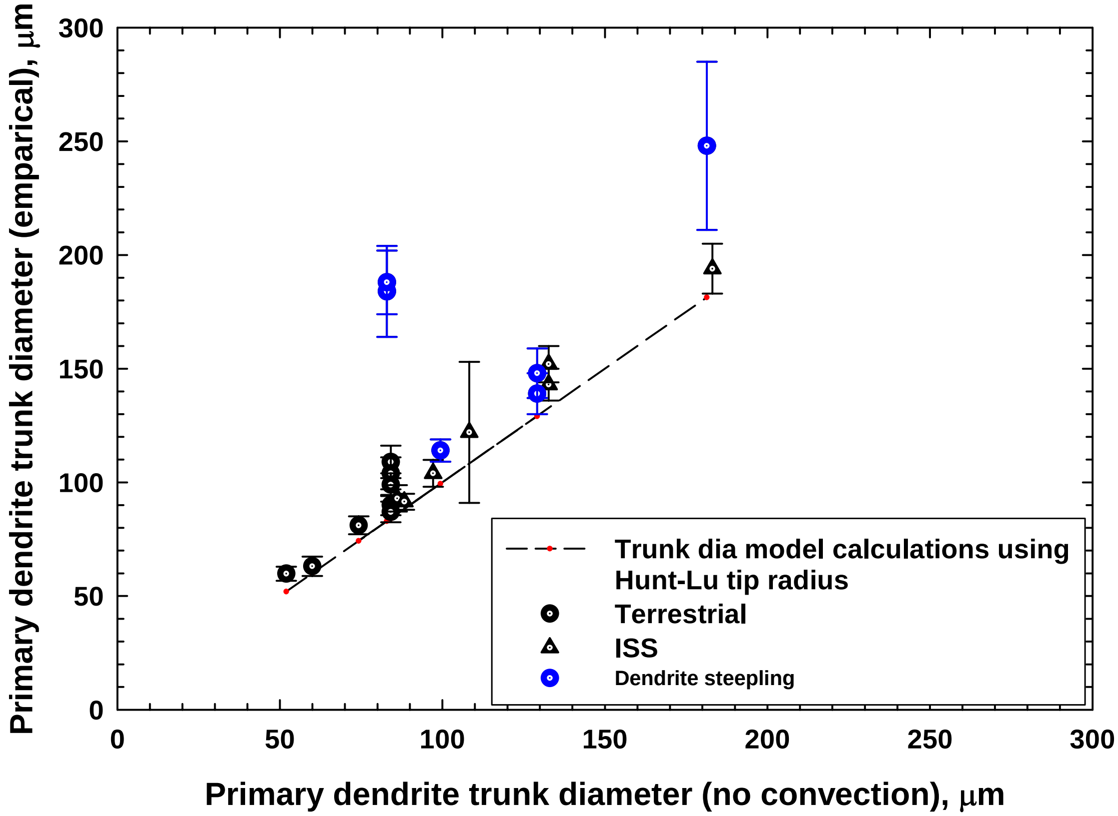

- ➢ISS-DS: Good agreement with predictions from the trunk-diameter model.
- ➢Terrestrial DS ("Not steepled") : Good agreement with predictions from model.
- ➢Terrestrial DS ("steepled"): Convection increases trunk diameter.

ISS samples show better agreement with calculations from the models than terrestrial samples (primary spacing and trunk diameter (Observed/Predicted)

	Trivedi		
	ISS-samples	Terrestrial (no steepling)	Terrestrial (steepling)
Primary dendrite arm spacing/calculated from model	0.945± 0.0833 (σ/μ=0.09)	0.791± 0.0931 (σ/μ= 0.12)	0.695± 0.223 (σ/μ=0.32)
Primary dendrite trunk diameter/calculated from model	1.069± 0.0361 (σ/μ= 0.05)	1.113± 0.0890 (σ/μ=0.08)	1.513± 0.560 (σ/μ=0.37)

SURPRISES??

MICAST-6: Grains elimination and formation along DS length

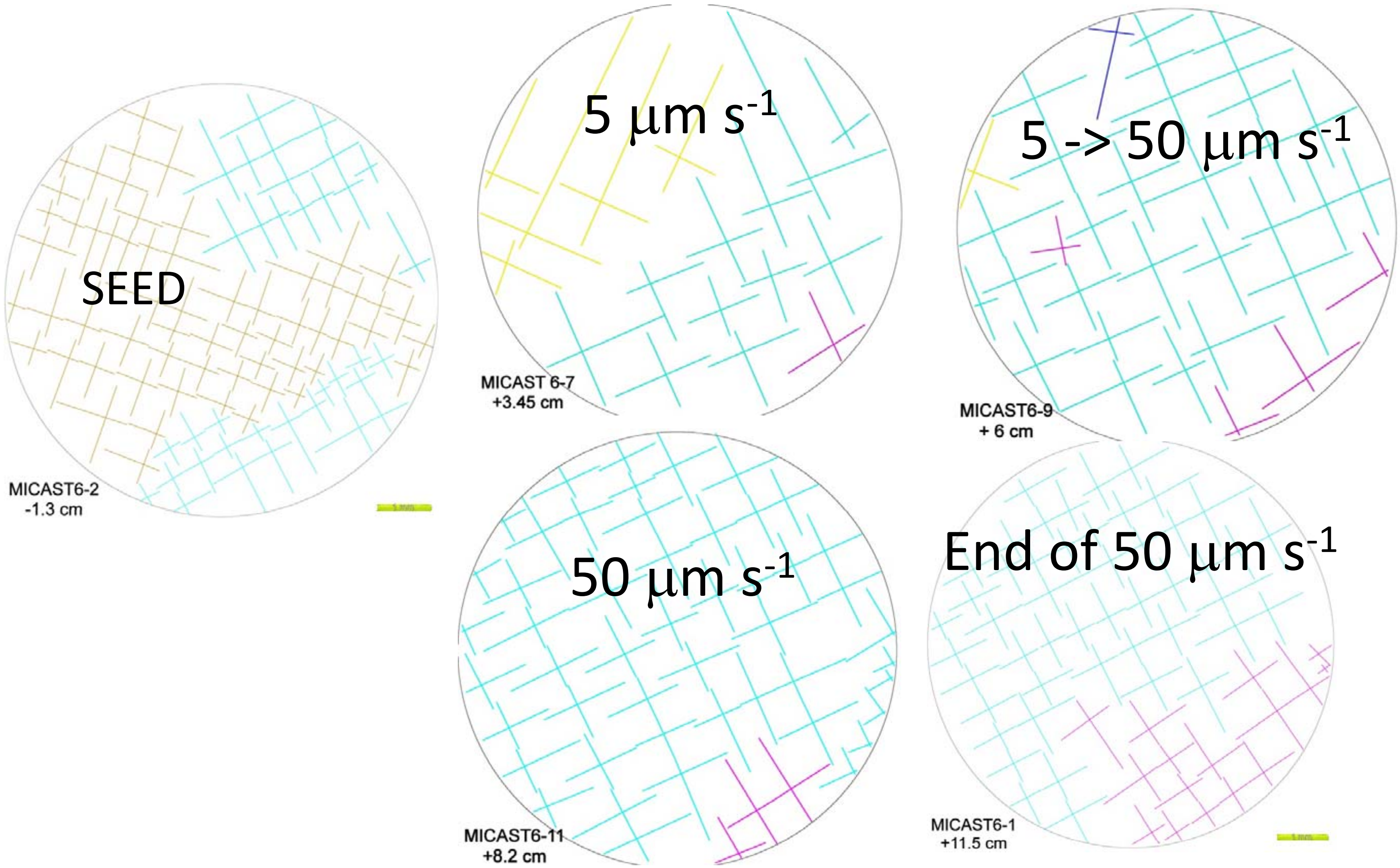

SPURIOUS GRAINS DURING DS IN THE ABSENCE OF CONVECTION ??

MICAST7-1T (Ground processed seed crystal)

Al – 7wt. % Si, $V = 22\ \mu m\ s^{-1}$, $G_l = 41\ K\ cm^{-1}$

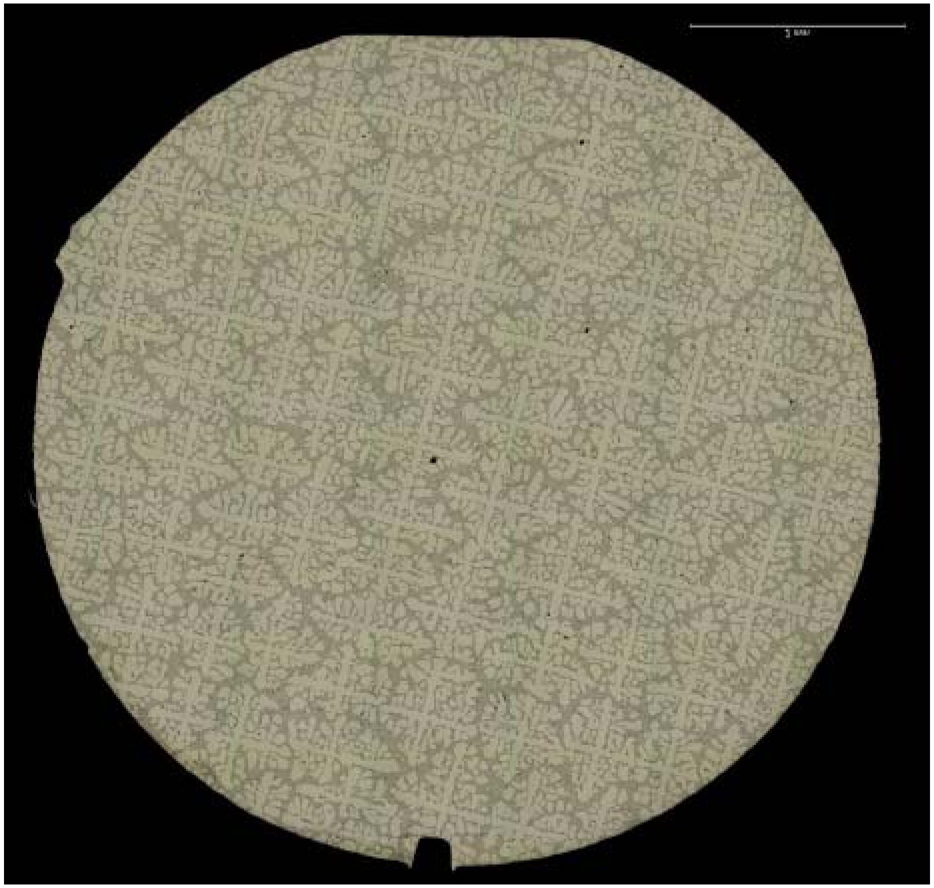

Transverse optical microstructure

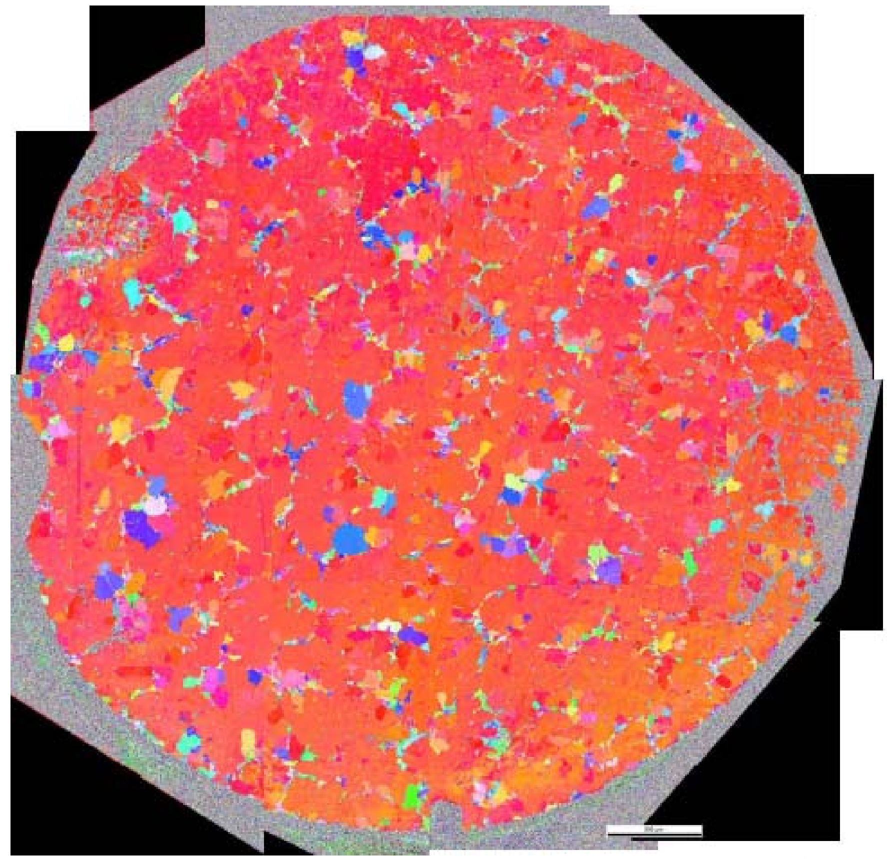

Composite EBSD Scan

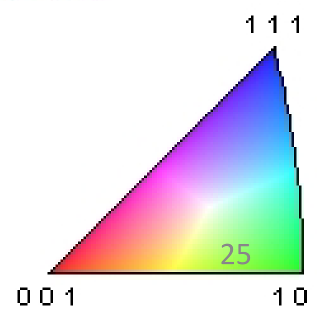

Very good [100] alignment, some spurious grains/arms

Microgravity Processed MICAST 7

MICAST7 – 3T (20 $\mu m\ s^{-1}$, G_l = 26 $K\ cm^{-1}$)

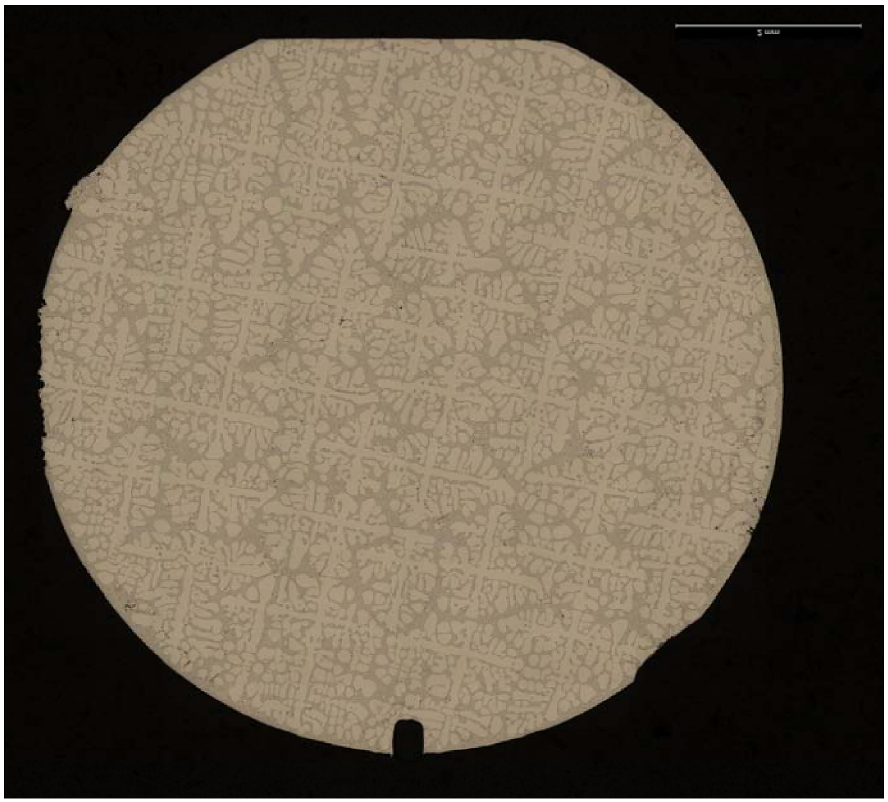

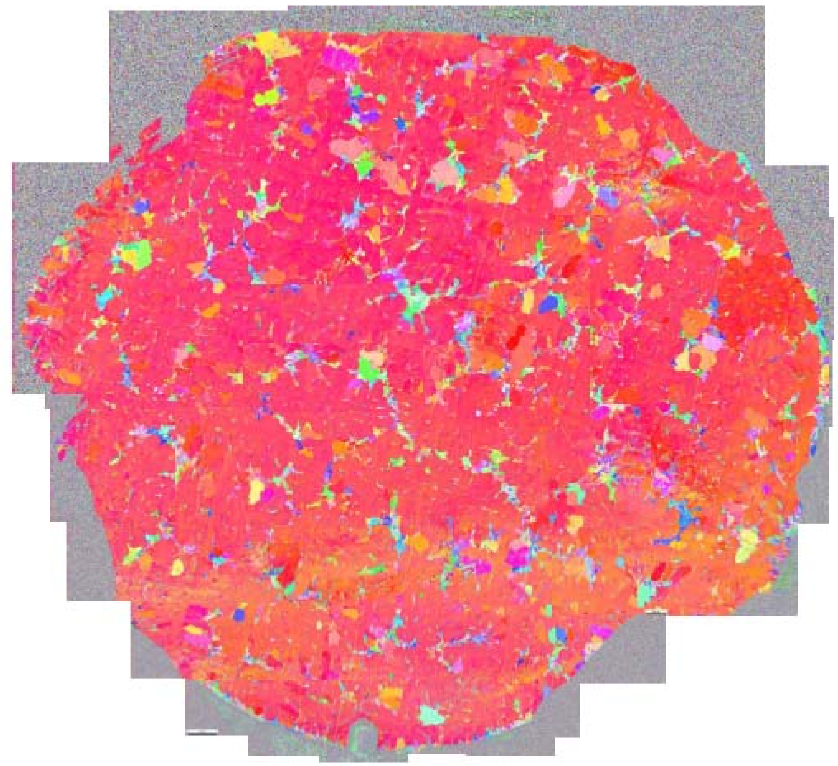

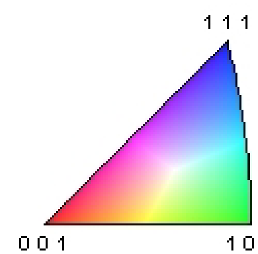

Very good (better) alignment, less spurious grains

Microgravity Processed MICAST 7

MICAST7 – 5T (10 μm s^{-1}, G = 28 K cm^{-1})

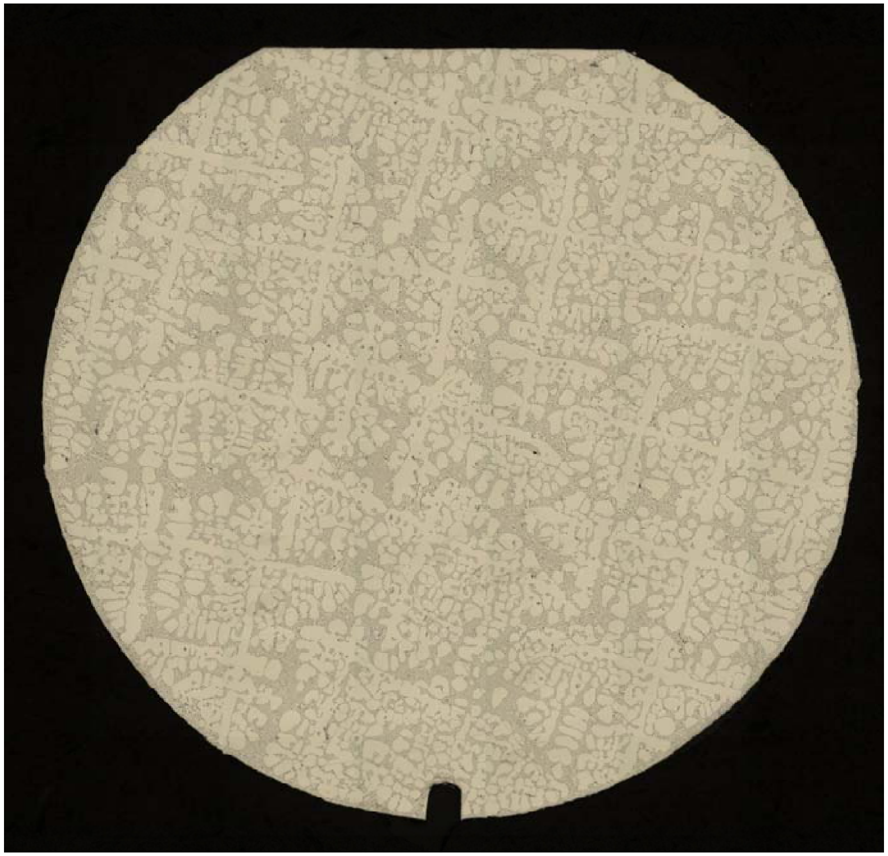

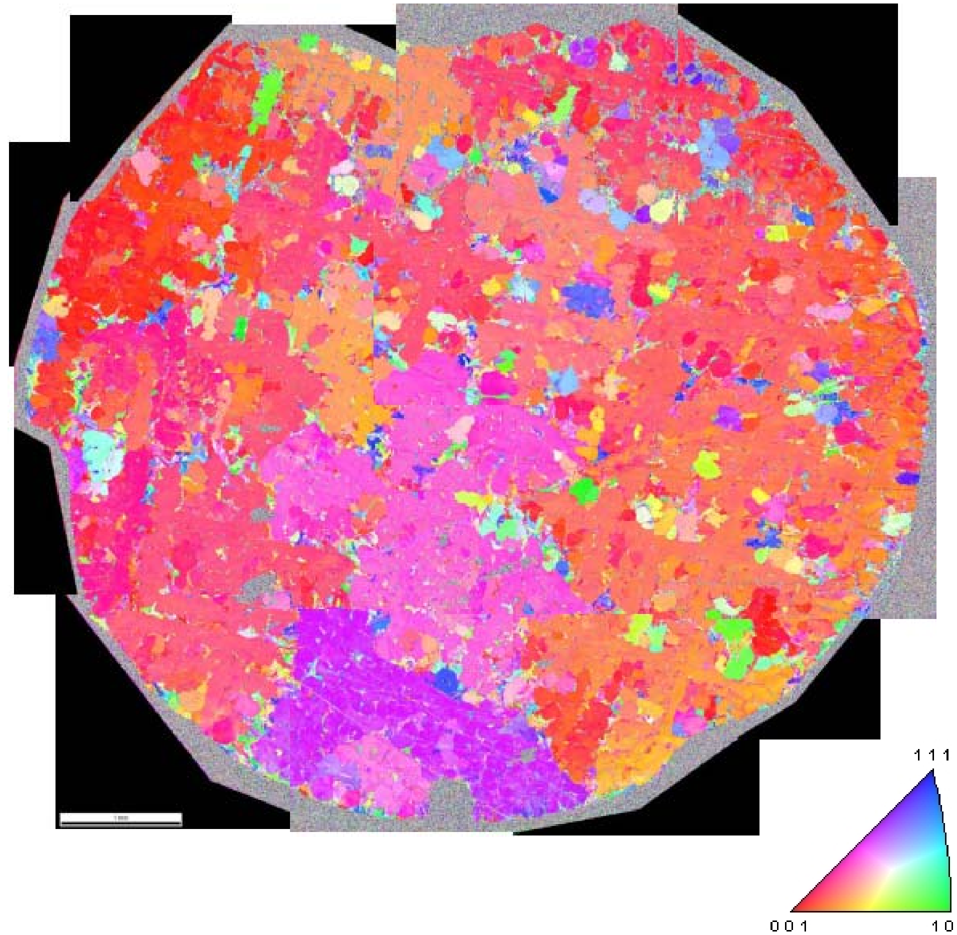

Very poor alignment, very many spurious grains

Conclusions

- Primary dendrite arm spacings of Al-7 wt% Si alloy directionally solidified in low gravity environment of space (MICAST-6 and MICAST-7: Thermal gradient ~ 19 to 26 K cm^{-1}, Growth speeds varying from 5 to 50 $\mu m\ s^{-1}$) show a good agreement with predictions from Hunt-Lu and Trivedi models.
- Primary dendrite trunk diameters of the ISS processed samples show a good fit with a simple analytical model based on Kirkwood's approach, proposed here.
- Natural convection,
  - decreases primary dendrite arm spacing.
  - appears to increase primary dendrite trunk diameter.
- Spurious grains formed during DS in "low-g<10^{-4} g"??

Acknowledgements

- NASA
- ESA
- DLR-MUSC
- ALCOA